Divergent $GABA_A$ Receptor-Mediated Synaptic Transmission in Genetically Seizure-Prone and Seizure-Resistant Rats

Dan C. McIntyre,[1] Bruce Hutcheon,[1,2] Kerstin Schwabe,[3] and Michael O. Poulter[1,2]

[1]Neuroscience Research Institute, Carleton University, Ottawa, Ontario, Canada K1S 5B6, [2]Laboratory of Molecular Neuropharmacology, Institute for Biological Sciences, National Research Council of Canada, Ottawa, Ontario, Canada K1A 0R6, and [3]Department of Pharmacology, Toxicology, and Pharmacy, School of Veterinary Medicine, D-30559 Hannover, Germany

Recent evidence suggests that abnormal expression of $GABA_A$ receptors may underlie epileptogenesis. We observed previously that rats selectively bred to be seizure-prone naturally overexpressed, as adults, GABA α subunits (α2, α3, and α5) seen at birth, whereas those selected to be seizure-resistant overexpressed the adult, α1 subunit. In this experiment, we gathered GABA miniature IPSCs (mIPSCs) from these strains and correlated their attributes with the subunit expression profile of each strain compared with a normal control strain. The mIPSCs were collected from both cortical pyramidal and nonpyramidal neurons. In seizure-prone rats, mIPSCs were smaller and decayed more slowly than in normal rats, which in turn were smaller and slower than in seizure-resistant rats. A detailed analysis of individual mIPSCs revealed two kinds of postsynaptic responses (those with monoexponential vs biexponential decay) that were differentially altered in the three strains. The properties of monoexponentially decaying mIPSCs did not differ between pyramidal and nonpyramidal neurons within a strain but differed between strains. In contrast, an interaction was observed between cell morphology and strain for biexponentially decaying mIPSCs. Here, the mIPSCs of pyramidal neurons in the seizure-resistant rats formed a distinct subpopulation compared with the seizure-prone rats; yet in the latter rats, it was the mIPSCs of the nonpyramidal neurons that were unique. Given these differences, we were surprised to find that the total inhibitory charge transfer between the strains was similar. This suggests that the timing of inhibition, particularly slow inhibitory neurotransmission between nonpyramidal neurons, may be a contributing factor in seizure genesis.

Key words: subunits; epilepsy; $GABA_A$ receptors; inhibitory currents; interneurons; perirhinal cortex

Numerous studies have shown that $GABA_A$ receptor behavior varies with subunit expression (Verdoorn et al., 1990; Angelotti and Macdonald, 1993; Verdoorn, 1994; Dominguez-Perrot et al., 1995; Zhu et al., 1995; Tia et al., 1996; Burgard et al., 1999; Haas and Macdonald, 1999; McClellan and Twyman, 1999; Hutcheon et al., 2000). From one brain region to the next, the genetic expression is diverse, giving rise to differing functional profiles of GABAergic inhibition that are hypothesized to control the rhythmicity of neural networks. This control of neural network rhythmicity is altered in many neurological disorders (Traub et al., 1999), including temporal lobe epilepsy (TLE).

Although the structural origins and expression of complex partial seizures in human TLE are varied, the hippocampus, amygdala, and adjacent cortical areas are thought to be significant contributors to the syndrome (Gloor, 1991). As a result, alterations in inhibition within these structures have been the focus of many studies. Recently, the search for a molecular basis of epilepsy has received strong, convergent support from several experimental models, suggesting that the expression of $GABA_A$ receptors in these brain areas is abnormal (Brooks-Kayal et al., 1998, 1999; Schwartzkroin, 1998; Sperk et al., 1998; Loup et al., 2000). Indeed, in our genetically based amygdala kindling models of TLE (Racine et al., 1999), we have shown that differential kindling rates (McIntyre et al., 1999) are correlated with differences in $GABA_A$ subunit expression (Poulter et al., 1999). In these models, a genetic predisposition to amygdala kindling in adult rats is correlated with an overexpression of the $GABA_A$ receptor subunits that normally predominate in the immature brain (α2, α3, and α5). Conversely, overexpression of the major adult α subunit (α1) is associated with resistance to kindling. Because GABA-mediated neurotransmission not only truncates action potential generation but also synchronizes and/or times the output of neural circuits (Whittington et al., 1995; Wang and Buzsaki, 1996), it has been suggested (Poulter et al., 1999) that the abnormal expression of certain $GABA_A$ receptors may result in the periodic failure of the brain to prevent excessive synchrony across neural networks.

The purpose of the present study was to correlate the electrophysiological properties of $GABA_A$ receptor-mediated synaptic transmission in rats that have different $GABA_A$ receptor subunit expression and predispositions to epileptogenesis. We have hypothesized that differences in subunit expression underlie altered neural network timing profiles and, in turn, seizure vulnerability. As a first step, we wanted to understand how the inhibitory synaptic currents are different in these different rat strains. To this end, we show for the first time that differing behaviors of $GABA_A$ receptor-mediated synaptic transmission are correlated to our previously reported subunit expression profiles (Poulter et al., 1999). These results suggest that the observed differences in

Received April 12, 2002; revised June 21, 2002; accepted Aug. 21, 2002.

This work was supported by the National Research Council of Canada and by the Canadian Institutes of Health Research.

Correspondence should be addressed to Dr. M. O. Poulter, Associate Professor, Neuroscience Research Institute, Department of Psychology, Carleton University, 1125 Colonel By Drive, Ottawa, Ontario, Canada, K1S 5B6. E-mail: michael_poulter@carleton.ca.

 0270-6474/02/229922-10$15.00/0

inhibitory activity between the strains may underlie both the seizure-prone and seizure-resistant phenotypes.

MATERIALS AND METHODS

All experiments were conducted in accordance with the guidelines of the Canadian Council on Animal Care and protocols approved by the Carleton University and National Research Council of Canada Animal Care Committees.

Animals. The seizure-prone and seizure-resistant rat strains were originally developed at McMaster University (Hamilton, Ontario, Canada) from an outbred parent population consisting of a Long–Evans hooded and Wistar cross (Racine et al., 1999). For 11 generations, these rats were selectively bred for their differential rates of amygdala kindling. The resulting two strains [called "Fast" and "Slow" by Racine et al. (1999)] now are bred nonselectively within each strain in a manner to preclude brother–sister or first-cousin pairings and are maintained at Carleton University. The seizure-prone and -resistant rats used in the present project were taken from generations 41–44. As "normal" rats, one of the original two parent strains (Long–Evans hooded) was used; they were purchased from Charles River Canada (St. Constant P.Q., Canada).

Electrophysiology. Patch-clamp recordings were performed on brain slices isolated from adult rats (60–200 d of age). To obtain viable slices, heavily anesthetized rats (sodium pentobarbital, 80 mg/kg, i.p.) were perfused with an ice-cold Ringer's solution in which sodium was replaced by choline (composition in mM: 110 choline Cl, 2.5 KCl, 1.2 NaH_2PO_4, 25 $NaHCO_3$, 0.5 $CaCl_2$, 7 $MgCl_2$, 2.4 Na pyruvate, 1.3 ascorbate, and 20 dextrose), thus cooling and neuroprotecting the brain *in situ*. Specifically, this was done by opening the thoracic cavity, clamping off the descending aorta, and cutting the right atrium. The left ventricle of the heart was subsequently punctured with an 18 gauge needle and perfused with 50 ml of the ice-cold choline solution. After perfusion, the brain was rapidly removed from the skull, and the temporal lobe area was excised as a block. The block was subsequently sliced (coronally) with a Vibratome (200- to 400-μm-thick sections). The slices were incubated at 35°C for 30 min and subsequently moved to a room-temperature bath, where they were maintained until needed. Slicing, incubation, and storage were all performed in the choline solution. The Ringer's solution used during electrical recordings was similar to the choline solution except that pyruvate and ascorbate were removed, equimolar NaCl replaced the choline Cl, and $CaCl_2$ and $MgCl_2$ were both used at a 2 mM concentration.

We used KCl patch electrodes having an internal composition (in mM) of 145 KCl, 10 NaCl, 2 $CaCl_2$, 10 EGTA (yielding a free Ca^{2+} concentration of 100 nM), 2 MgATP, 10 dextrose, and 10 HEPES (300–320 mOsm; pH adjusted to 7.3–7.4). The input resistance of these electrodes was 3–8 MΩ, and their shanks were coated in beeswax to reduce electrode capacitance. Recordings from neurons in layers 3 and 5 of the perirhinal cortex were made with an Axopatch 200B amplifier (Axon Instruments, Carver City, CA). Series resistance compensation was performed in all recordings. Acceptable recordings were those in which the initial access resistance was <20 MΩ and could be compensated by 70–80% (100 μsec lag). The series resistance was monitored throughout the recordings, and if it rose irreversibly above 20 MΩ, the recording was terminated. Under these conditions and on the basis of the size of the currents monitored (20–200 pA), the remaining uncompensated series resistance caused a voltage error of <1%, whereas filtering errors were negligible.

Neurons were visualized with differential interference contrast optics. Both voltage-clamp and current-clamp recordings were made to compare the voltage-gated membrane currents and excitability. Spontaneously occurring miniature IPSCs (mIPSCs) were collected in the presence of 200–500 nM tetrodotoxin (TTX; Alomone Laboratories, Tel Aviv, Israel), 10 μM dinitroquinoxaline-2,3-dione (DNQX; Research Biochemicals, Natick, MA), and 20 μM 2-amino phosphonopentanoic acid (APV; Research Biochemicals). Recordings were performed at room temperature (22–26°C), because at higher temperatures, mIPSCs arrived too quickly and were rarely separated from one another enough to permit useful fitting and analysis. Putative mIPSCs were acquired as brief, negative-going transients in the current necessary to hold the membrane potential at −60 mV.

Analysis of mIPSCs. The deactivation phases of the mIPSCs were individually fitted with exponential functions. Monoexponential and biexponential fits were performed on each mIPSC. The residual deviations were subsequently compared to decide which fit to retain, as described by Hutcheon et al. (2000). Fits and subsequent sorting and analysis of the data were performed automatically by use of the macro facility in Clampfit (Axon Instruments) and a macro written in house in Visual Basic to control the operations of Microsoft (Redmond, WA) Excel worksheets. In all analyses, mIPSCs were sorted to eliminate events with 10–90% rise times of >1.5 msec, half-width durations of <4 msec (i.e., events that were too brief to be considered genuine GABAergic synaptic transients), and events that were not considered to be caused by a single mIPSC. After sorting by these criteria, ~80% of the collected events were rejected [i.e., ~30% of the mIPSCs had rise times that were >1.5 msec, ~40% could not be fitted because another mIPSC occurred during the fitting window, and ~10% were false events (shifts in the baseline)].

For comparisons between rat strains and morphological cell type, 45–65 mIPSCs were randomly selected from the recordings of each cell, and the parameter values derived from the corresponding individual fits were pooled with those of other cells. Limiting the number of mIPSCs from each cell in this way ensured that each neuron was equally represented in the analysis while preserving the variability of the measured attributes. Because our criteria for automated sorting were highly conservative, some recordings had too few mIPSCs to be included in this part of the analysis, although they could be retained in other analyses (averaging; see below). For this reason, the number of cells from the individual mIPSC analysis is not the same as that for the data in which an average of the mIPSCs was calculated.

This initial analysis permitted the comparison of attributes of the individual mIPSCs within strains (on the basis of their pyramidal and nonpyramidal cell morphology) and between strains by generating six different distributions: (1) time constants of monoexponential mIPSCs and (2) their amplitudes; (3) the fast and (4) the slow time constants of deactivation of biexponential mIPSCs and (5) their amplitudes; and (6) the percentage component of fast deactivation of the biexponential mIPSCs. None of these quantities were normally distributed (as determined by Kolmogorov–Smirnov normality tests); hence, all representative data are reported as medians with interquartile ranges.

Statistical tests were performed to detect differences in the median values of data from the same morphological cell types in the three different strains. That is, data from pyramidal neurons in one strain were tested against pyramidal neurons in the other strains but not against data from nonpyramidal neurons. For statistical comparisons of the medians, a Kruskal–Wallis test was first used with a level of significance set at $p = 0.01$. If a significant difference between medians was detected, then *post hoc* comparisons between individual medians were calculated on the basis of Dunn's test. Mann–Whitney *U* tests were used to detect differences in the median values of pyramidal and nonpyramidal neurons in the same strain.

To provide insight into how simultaneous mIPSCs might be combined in neurons, 50–100 individual events were chosen in each cell, aligned by their rising phases (<1.5 msec), and averaged together. The resulting signals, denoted by a subscripted and appended "av" (hence, $mIPSC_{av}$), then had their declining phases fitted with sums of exponentials as in the analysis of individual mIPSCs described above. This yielded one set of fitted parameters per neuron. These averages for individual neurons were subsequently grouped by rat strain and cellular morphology to yield categorized distributions of the parameters. Because these distributions were found to be normal, they are summarized throughout as means ± SEM. A one-way ANOVA was used to test for differences in means between similar cell types in different strains (significance level, $p = 0.01$). If a difference was detected, a Newman–Keuls *post hoc* test was used to compare individual means. Differences between the attributes of pyramidal and nonpyramidal neurons in the same strain were detected using Student's *t* tests.

Histocytochemistry. Cells from which recordings were made were filled with 0.5% biocytin (Sigma-Aldrich, Oakville, Ontario, Canada) and subsequently visualized by streptavidin conjugated to the fluorescent 6-((7-amino-4-methylcoumarin-3-acetyl)amino hexonic acid molecule (Jackson ImmunoResearch, West Grove, PA). A series of digital photos in the *z*-axis (1.5 μM apart) were taken with a Photometrics Star 1 camera (25× magnification; 580 × 380 pixel resolution). The stack of images was subsequently deconvolved using a commercially available software package (Exhaustive Photon Reassignment; Scanalytics, McClean, VA). The entire cell morphology was visualized by projecting the deconvolved optical sections onto a single plane. Background and imperfections were subtracted or retouched using Corel (Ottawa, Ontario, Canada) Photopaint to produce a final duotone image. Classification of the cells as

either pyramidal or nonpyramidal was based on the morphology of the soma, the existence and orientation of a dominant dendrite, and the projection of the axon.

RESULTS

Using brain slices obtained from adult normal, seizure-prone, or seizure-resistant rat strains (Racine et al., 1999), we made recordings from >300 neurons in the perirhinal cortex, a structure that has been strongly implicated in the secondary generalization of limbic-kindled seizures (Kelly and McIntyre, 1996; Ferland et al., 1998) and in which the magnitude and timing of inhibition is probably very important. Recordings were selected for analysis on the basis of the criteria stated in Materials and Methods (low-access resistance and adequate resistance compensation). These recordings were subsequently selected for inclusion in the results reported below only if the morphology of the neuron could be ascertained (see Materials and Methods). On the basis of these criteria, this gave 82 recordings that are described below.

We found that whole-cell recordings from neurons in layers 3 or 5 of the perirhinal cortex showed similar voltage–current properties across the different rat strains. Although the high synaptic activity and spontaneous action potential generation often made it difficult to reliably characterize the spiking properties in many recordings, we identified rapidly accommodating, fast, regular, and intermittent spiking, and occasionally bursting neurons in all three strains. The average resting membrane potentials for neurons in all three strains were similar (approximately −65 mV). The membrane time constants, measured with hyperpolarizing current pulses near the resting potential, were also the same between strains and were fit by the sum of two exponentials, one ~2–4 msec and the other ~50–80 msec.

Averaged time courses of miniature synaptic events (mIPSC$_{av}$s)

In the presence of TTX (200–500 nM), DNQX (10 μM), and APV (20 μM), we collected mIPSCs while maintaining the neurons at a holding potential of −60 mV. The mIPSCs were clearly mediated by activation of $GABA_A$ receptors, because they were blocked by the application of either 10 μM gabazine or 20 μM bicuculline (10 of 10 cells).

For each neuron, after collecting sufficient mIPSCs, we constructed an averaged time course (mIPSC$_{av}$) as described in Materials and Methods. This traditional method of analysis increases the signal-to-noise ratio in the synaptic signal for the purposes of determining synaptic kinetics. A drawback is that the actual nonstochastic variability between individual synaptic signals may be masked by the averaging procedure. On a different level, however, the mIPSC$_{av}$ may be understood as an idealized representation of synaptic integration such as would result from a synchronous activation of $GABA_A$ergic synapses.

As depicted in Figure 1, mIPSC$_{av}$s from the three different strains were readily distinguished on the basis of their size and time course of decay. To quantify these differences, we fitted exponential functions to the declining phase of mIPSC$_{av}$s. The majority of mIPSC$_{av}$s were best fitted by the sum of two exponential components. Table 1 gives the means of the parameter values obtained from these biexponential fits after grouping by strain and morphological cell type. It can be seen that the mIPSC$_{av}$s of both seizure-resistant and seizure-prone strains differed significantly from those of normal rats in the values of their fast (τ_1) and slow (τ_2) time constants for decay and in their amplitudes.

The attributes of seizure-resistant and seizure-prone rats diverged in opposite directions from those of normal rats. That is, parameter values obtained from the exponential fits to mIPSC$_{av}$s in normal rats were intermediate to those of seizure-resistant and seizure-prone rats. Overall, mIPSC$_{av}$s from neurons encountered in seizure-resistant rats were larger and decayed more quickly than those from normal rats, and these in turn were larger and decayed more quickly than those from seizure-prone rats (Fig. 1, Table 1).

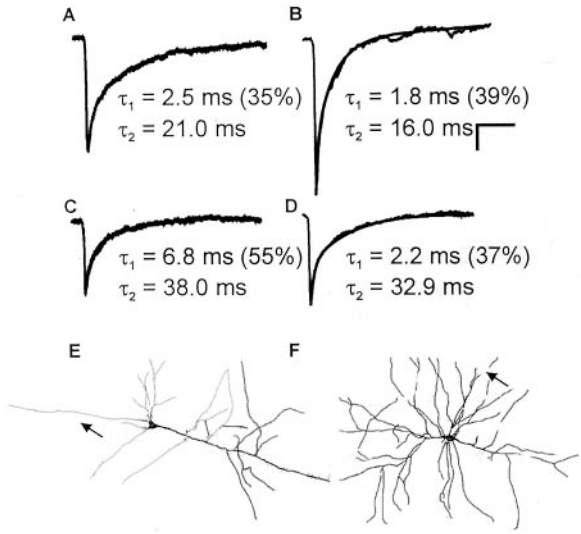

Figure 1. Examples of average mIPSCs from a normal rat (*A*), a seizure-resistant rat (*B*), a seizure-prone rat nonpyramidal neuron (*C*), and a seizure-prone rat pyramidal neuron (*D*). Each example shows the basic characteristics found in each strain. In seizure-resistant rats, the average time course was faster and the amplitude larger than in normal rats. Within each of these strains, both pyramidal and nonpyramidal neurons had similar mIPSC$_{av}$s. In contrast, in seizure-prone rats, the average time courses were slower and the synaptic events smaller than in normal rats. This was more pronounced in the nonpyramidal population (see Table 1 for summary). In *E* and *F*, we show examples of the morphological reconstructions that were done for all recordings. *E*, Typical neuron that was classified as pyramidal; *F*, example of one kind of nonpyramidal cell morphology, which as expected was more variable in morphology than pyramidal. Calibration: 10 msec, 10 pA. The *smooth line* through each average time course shows the fitted time course. *Arrows* indicate axonal projection.

We also directly compared the properties of mIPSC$_{av}$s in pyramidal versus nonpyramidal neurons in each strain. This comparison showed that in normal and seizure-resistant rats, the averaged synaptic time courses for these two cell types were statistically similar ($p > 0.25$ for all comparisons of fitted parameters). This was not true in seizure-prone rats, in which the average synaptic time courses measured in pyramidal and nonpyramidal cells were clearly different ($p < 0.03$). In this case, mIPSC$_{av}$s in pyramidal neurons decayed significantly faster than those of nonpyramidal neurons. In contrast, the amplitudes of mIPSC$_{av}$s did not differ between pyramidal and nonpyramidal neurons within a strain ($p > 0.3$; although, as stated above, there were large differences between strains).

Time courses of individual miniature synaptic events

We also examined the properties of individual mIPSCs from normal, seizure-resistant, and seizure-prone rats. The decay phase of each mIPSC in the database was fitted with a sum of exponentials, and the calculated parameters were pooled by strain and morphological type as described in Materials and Methods. Using this analysis we found that, in almost all neurons, two

Table 1. Comparison of $mIPSC_{av}$ attributes in morphologically identified neurons of seizure-resistant, normal, and seizure-prone rat strains

	Strain, cell type						
	Seizure-resistant		Normal		Seizure-prone		
	Pyramidal	Nonpyramidal	Pyramidal	Nonpyramidal	Pyramidal	Nonpyramidal	
Number of cells	15	12	15	9	15	12	4[b]
τ_1 (msec)	1.7 ± 0.13*	1.6 ± 0.1	2.4 ± 0.2	2.1 ± 0.2	3.0 ± 0.7*	5.1 ± 0.5***	
τ_2 (msec)	20.3 ± 1.0***	21.0 ± 0.8	24.2 ± 2.5	24.3 ± 2.4	27.7 ± 3.4*	39.9 ± 5.2***	26.6 ± 6.7
% τ_1[a]	40.0 ± 5.1	30.0 ± 2.9	40.0 ± 2.5	30.0 ± 6.7	40.0 ± 2.5	46.7 ± 4.5	
Amplitude (pA)	−57.3 ± 4.0***	−59.8, 3.6*	−44.6 ± 3.7	−51.7 ± 5.2	−39.7, 3.8	−34.0 ± 4.1*	−29.4

Values are mean ± SEM.

[a] Percentage of deactivation time course devoted to fastest time constant.

[b] Neurons identified as having monoexponentially decaying $mIPSC_{av}$s.

Significance with respect to neurons of the same morphology in normal rats: *$p < 0.05$; **$p < 0.01$; ***$p < 0.001$.

Table 2. Comparison of mIPSC attributes in morphologically identified neurons of seizure-resistant, normal, and seizure-prone rat strains

	Strain, cell type					
	Seizure-resistant		Normal		Seizure-prone	
	Pyramidal	Nonpyramidal	Pyramidal	Nonpyramidal	Pyramidal	Nonpyramidal
Number of cells	13	12	13	9	13	11
Monoexponential						
τ_1 (msec)	11.6,14.3**	12.1,13.0**	14.4,15.9	15.7,17.1	17.1,18.8**,***	21.6,23.4**,***
Amplitude (pA)	−39.9,35.0**	−39.0,27.1*	−32.7,25.8	−35.9,23.4	−26.3,24.6**,***	−27.8,17.0**,***
Number of events	750	533	634	500	560	534
Biexponential						
τ_1 (msec)	1.7,0.8*	1.6,0.7	2.3,1.1	1.7,0.8	2.6,1.1***	4.4,1.5**,***
τ_2 (msec)	26.3,9.8**	25.8,9.4	35.0,12.9	31.5,10.8	35.8,12.6***	51.6,20.1**,***
% τ_1	42.4,11.9	41.3,11.7	42.9,11.5	35.2,9.9	43.6,10.5	44.9,10.1**
Amplitude (pA)	−74.1,43.6**	−60.3,18.9	−49.3,13.8	−56.0,15.4	−43.1,24.7***	−36.2,14.5**,***
Number of events	200	163	189	149	187	157

Values are median, interquartile range.

[a] Percentage of deactivation time course devoted to fastest time constant.

Significance with respect to neurons of the same morphology in normal rats: *$p < 0.01$; **$p < 0.001$.

Significance with respect to neurons of the same morphology in seizure-resistant rats: ***$p \ll 0.001$.

populations of mIPSCs existed: those having monoexponential decay kinetics and those having biexponential decay kinetics. As in the analysis of $mIPSC_{av}$s described above, this analysis revealed marked differences between the strains (Table 2). We now show that the differences in monoexponential and biexponential kinetics are directly responsible for the differences in $mIPSC_{av}$s noted above, because the relative proportions of these two populations of synaptic events were similar (~3:1) across all strains and cell types (a single exception is described in a separate section below).

Monoexponential mIPSCs, which constitute the most common type of synaptic behavior in each neuron, exhibited highly significant differences in all possible comparisons between strains (Table 2). In contrast, the biexponential mIPSCs showed more restricted differences. Specifically, pyramidal neurons of seizure-resistant rats had larger, more quickly decaying biexponential mIPSCs than those of normal rats, but there was no such difference between nonpyramidal neurons. Conversely, in seizure-prone rats, nonpyramidal neurons had smaller, more slowly decaying mIPSCs than in normal rats, but there was no such difference in the pyramidal neurons (Fig. 2).

Within-strain comparison of mIPSC attributes in pyramidal and nonpyramidal neurons

Inhibition-related differences in seizure generation in the strains may depend more on the relative balance of inhibitory properties on pyramidal and nonpyramidal neurons than on strain-to-strain differences of the cell types. We therefore performed within-strain statistical comparisons of the attributes of mIPSCs in pyramidal and nonpyramidal neurons. In normal rats, we found no significant differences in the properties of mIPSCs on pyramidal and nonpyramidal neurons. Seizure-resistant rats similarly showed few differences, with the exception that the biexponential mIPSCs in pyramidal neurons were ~25% bigger than those in nonpyramidal neurons ($p < 0.01$). Seizure-prone rats, in contrast, had many differences in the attributes of their mIPSCs recorded from pyramidal and nonpyramidal neurons. Specifically, in the seizure-prone strain, the biexponential mIPSCs were larger in pyramidal neurons than in nonpyramidal neurons ($p < 0.001$), and both monoexponential and biexponential mIPSCs decayed more quickly in pyramidal neurons than in nonpyramidal neurons (monoexponential, $p < 0.001$; biexponential, $p < 0.03$ and

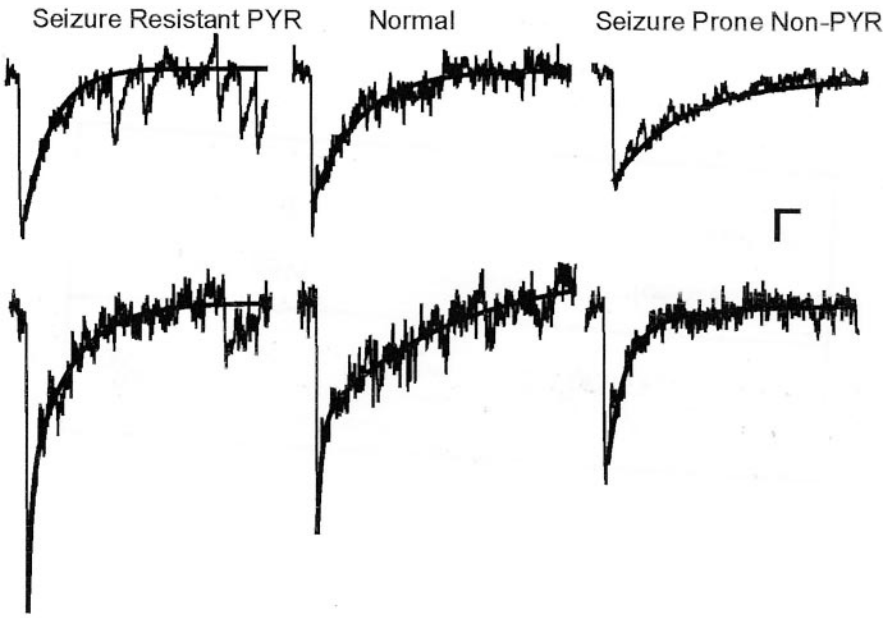

Figure 2. Two kinds of synaptic responses identified in nonpyramidal (*Non-PYR*) and pyramidal (*PYR*) neurons of all strains. Here, we show individual representative monoexponential (*top*) and biexponential (*bottom*) mIPSCs in seizure-resistant (pyramidal neuron), normal (pyramidal neuron), and seizure-prone (nonpyramidal neuron) rats. The mIPSCs were chosen to have attributes corresponding to the median values (amplitude and time course) found in each population. Calibration: 10 msec, 10 pA. The *smooth line* through each mIPSC shows the fitted time course. For illustration here, the fit window for each mIPSC was adjusted so that other events did not affect the fit of deactivation phase.

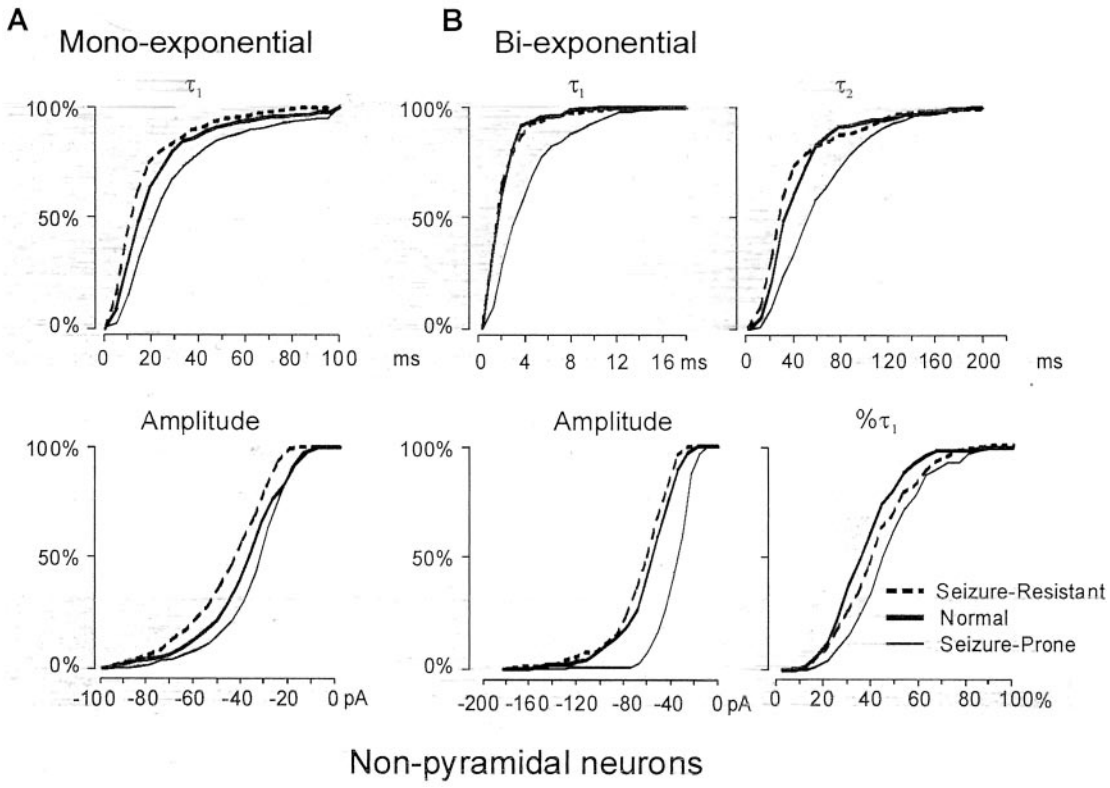

Figure 3. Cumulative distributions for the fitted attributes of mIPSCs from nonpyramidal neurons in each strain. The distribution of values for the seizure-prone rats is consistently different from those of normal and seizure-resistant rat strains, which tend to be similar to each other (see Table 2 for summary).

$p < 0.001$ for the fast and slow τ values, respectively). The amplitudes of monoexponential events did not differ significantly ($p > 0.1$).

Between-strain comparisons of mIPSC attributes

Because significant within-strain differences were detected between the attributes of mIPSCs in pyramidal and nonpyramidal neurons (see previous section), we separated the between-strain comparisons on the basis of cell morphology. We first compared mIPSCs in nonpyramidal neurons in the different strains. The results are highlighted by the cumulative distributions of fitted monoexponential and biexponential parameters for mIPSC decays shown in Figure 3. Statistical significance and summary measures are given in Table 2. Although there was substantial variability in the values of most parameters, differences in the

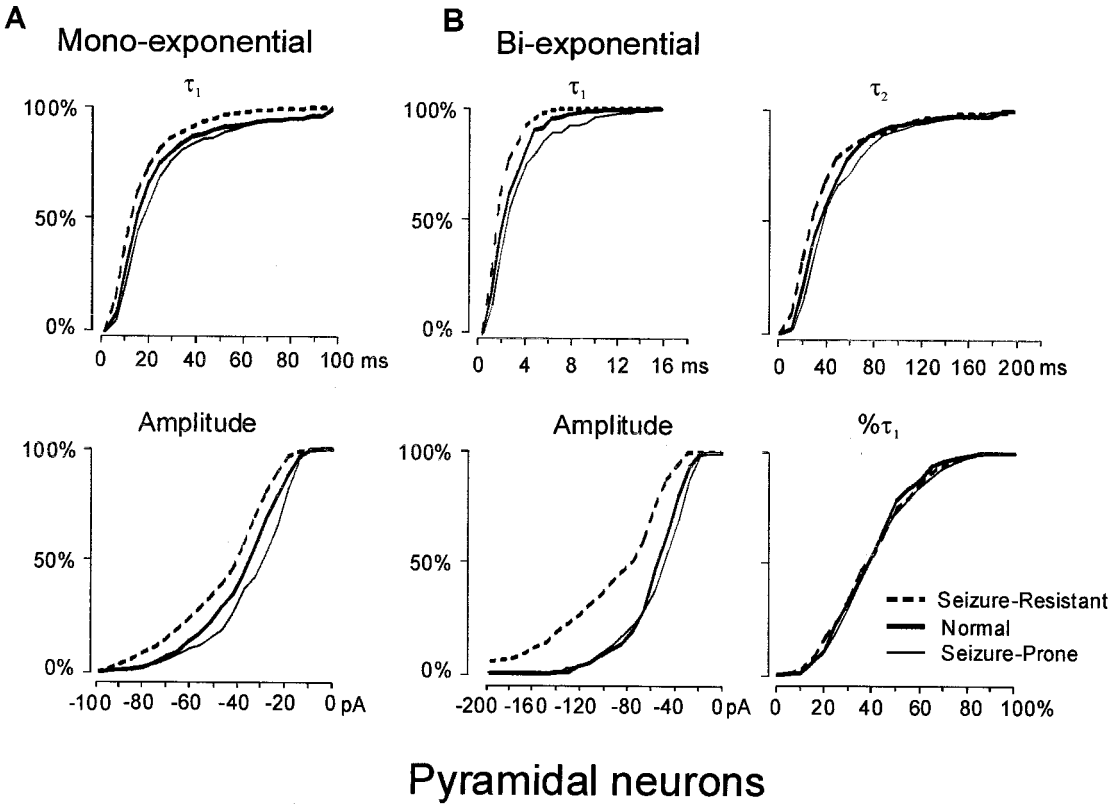

Figure 4. Cumulative distributions for the fitted attributes of mIPSCs from pyramidal neurons in each strain. In contrast to the situation for nonpyramidal neurons, the distributions of attributes for seizure-resistant rats were distinct from those of either normal or seizure-prone rats, which tended to be similar (see Table 2 for summary).

cumulative distributions are evident. For monoexponentially decaying mIPSCs, all possible comparisons showed significant differences following the overall trend that mIPSCs in seizure-resistant rats were larger and more quickly decaying than those in normal rats, which, in turn, were larger and more quickly decaying than those in seizure-prone rats. For biexponentially decaying mIPSCs in nonpyramidal neurons, only the seizure-prone rats formed a distinctive population, because they had smaller, more slowly decaying synaptic signals than the other two strains. There were no corresponding significant differences between seizure-resistant and normal rat strains.

Partially contrasting results were obtained when pyramidal cell mIPSCs were compared across strains (Fig. 4, Table 2). Once again, for monoexponential mIPSCs, all possible comparisons between strains showed statistically significant differences, with the same relative trends as for the nonpyramidal neurons. For biexponential mIPSCs, however, differences were restricted to seizure-resistant rather than seizure-prone rats, as was the case for nonpyramidal neurons. Thus, for pyramidal neurons, it is the seizure-resistant rats that had a distinctive population of biexponentially decaying mIPSCs, in this case a population of large, quickly decaying synaptic signals.

Overall, then, and in common with the earlier analysis of $mIPSC_{av}$s, we found that the parameter values characterizing mIPSCs in seizure-resistant and seizure-prone rats diverged from each other, with normal rats presenting intermediate values. This was true in both pyramidal and nonpyramidal neurons and for monoexponentially and biexponentially decaying mIPSCs. The only extracted parameter for which this was not true was the percentage of the total signal devoted to the fast component of decay, which for the most part, did not vary systematically between strains. Differences between the strains, however, were found to be concentrated in different neuronal populations. Seizure-resistant rats had a special set of biexponentially decaying mIPSCs in their pyramidal neurons, whereas seizure-prone animals had a special set of biexponentially decaying mIPSCs in their nonpyramidal neurons.

Monoexponential and biexponential mIPSCs are distinct populations

A potential problem with the above analysis is the possibility that many small-amplitude, monoexponential mIPSCs are really misclassified biexponential mIPSCs (i.e., fittings may periodically fail because of a low signal-to-noise ratio). To test this possibility, we reduced the signal-to-noise ratio by decreasing the amplitude of mIPSCs ~20% using a low dose (2–5 μM) of bicuculline. In agreement with the hypothesis that misclassifications in fact were rare, we found that there was no statistical difference ($p > 0.05$) in the relative proportion of monoexponential versus biexponential events after exposure to bicuculline. Thus, there was a high degree of tolerance in the fitting routines. Moreover, bicuculline did not alter the kinetics of the mIPSCs [control series: monoexponential, τ = 13.8, 11.2 msec (median, intraquartile range); biexponential, τ_1 = 3.4, 0.9 msec, τ_2 = 35.5, 5.5 msec; bicuculline series: monoexponential, τ = 14.4, 16.7 msec; biexponential, τ_1 = 3.3, 1.3 msec, τ_2 = 35.6, 17.8 msec; n = 5 cells; $p > 0.05$ for all comparisons]. Overall, these data indicate that in perirhinal neurons, monoexponential and biexponential synaptic transients arise either from synapses with distinct types of $GABA_A$ recep-

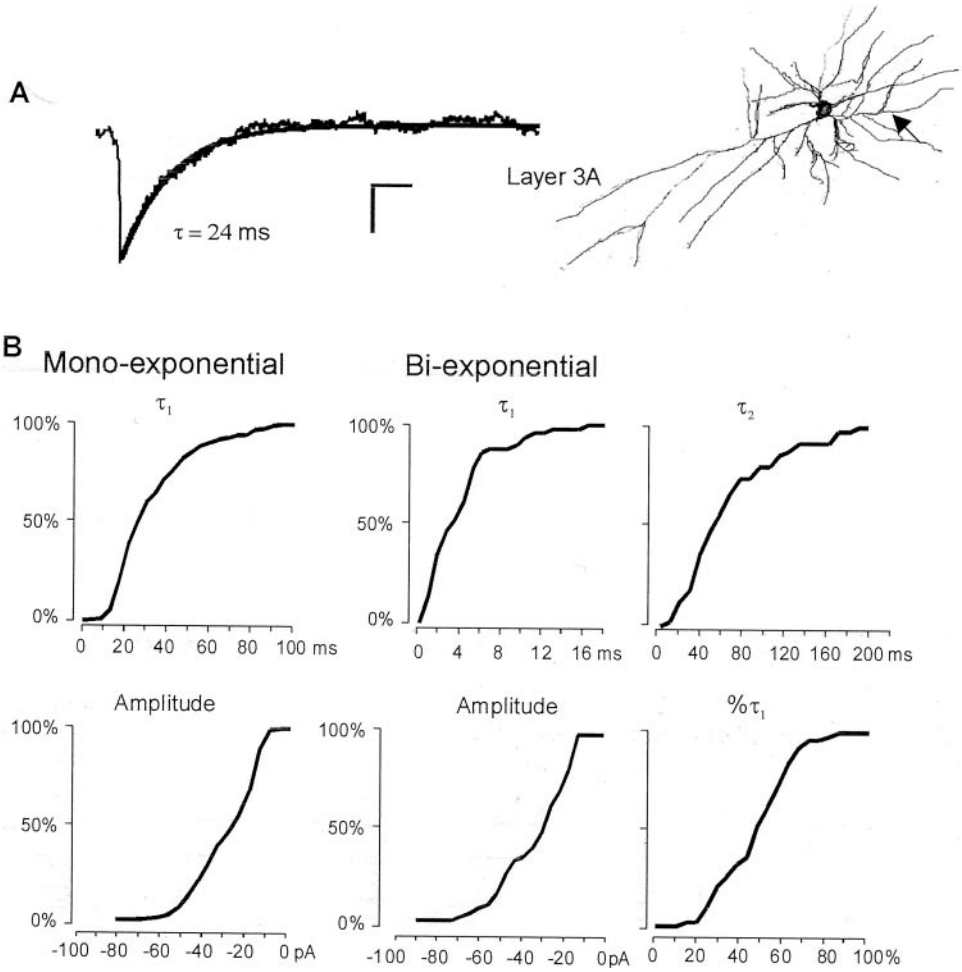

Figure 5. Analysis of amplitude and deactivation kinetics for GABAergic mIPSCs recorded from a subpopulation of four nonpyramidal neurons in a seizure-prone strain. *A*, In contrast to most other recordings in normal and seizure-resistant rats, the averaged mIPSCs from this population were small and deactivated with a monoexponential deactivation time course. *B*, The cumulative data for mIPSC attributes in these four recordings show an underrepresentation (10% compared with 25–35% in other recordings) of biexponential events. Also, there was no difference in the mIPSC amplitudes for the two types of events ($p > 0.05$). Thus, the summated inhibition in these cells arises from a predominance of one population of events over the other. The *arrow* indicates axonal projection.

tors or synapses with the same receptor in different functional states.

A unique population of nonpyramidal neurons in seizure-prone rats

In one population of nonpyramidal cells from seizure-prone rats, $mIPSC_{av}$s decayed with a single exponential component ($n = 4$) (Fig. 5). The mean value of the exponential decay time constant in these cells was similar to the values of the slower biexponential decay time constant in the pyramidal neurons in seizure-prone rats (Table 1). Two additional neurons from seizure-prone rats also had monoexponential kinetics, although in these cases, we were unable to determine their somatic morphologies. In contrast, in the other 64 morphologically identified recordings from the other two rat strains (and another 100 or so others without morphological identification), only one cell from a normal rat and none from seizure-resistant rats had an $mIPSC_{av}$ with monoexponential deactivation. An analysis of individual events was also performed on the four recordings with monoexponential $mIPSC_{av}$s as described above. In contrast to all other neurons encountered, in these nonpyramidal neurons from seizure-prone rats, ~90% of the mIPSCs had monoexponential decays. This represents a substantial subpopulation of neurons in the seizure-prone strain of rats (4 of 19 identified recordings) having distinctive synaptic kinetics that appears to be rare or perhaps nonexistent in the normal or seizure-resistant strains, respectively.

Time course of the synaptic signal versus charge transfer

To isolate the properties of inhibitory synaptic signaling that are most likely to cause functional differences between normal, seizure-resistant, and seizure-prone rats, we first calculated the charge transfer during the decay phase of the $mIPSC_{av}$s for the three different strains and two morphological cell types. In normal and seizure-resistant rats, the charge transfers for pyramidal and nonpyramidal neurons were not calculated separately, because their attributes were shown previously to be statistically similar. The results are shown graphically in Figure 6, which also includes calculated charge transfers for the four nonpyramidal neurons in seizure-resistant rats whose synaptic decay was primarily monoexponential. Surprisingly, despite the strain-dependent differences in peak amplitudes of $mIPSC_{av}$s, the mean total charge transfer showed no significant variation between strains (Fig. 6*A*). Functional differences in $GABA_A$ergic signaling between the strains therefore do not arise simply from each synapse delivering either more or fewer negative ions into neurons when stimulated.

We also reconstructed representative time courses of $GABA_A$ergic signaling using the mean values of $mIPSC_{av}$s from Table 1. Figure 6*B* plots the instantaneous deviations of the reconstructed synaptic currents from the normal strain. This shows that the strains differ markedly during the early period of the synaptic signal (<10 msec) (Fig. 6*B*). During this initial interval, synapses in neurons from seizure-prone rats pass far less

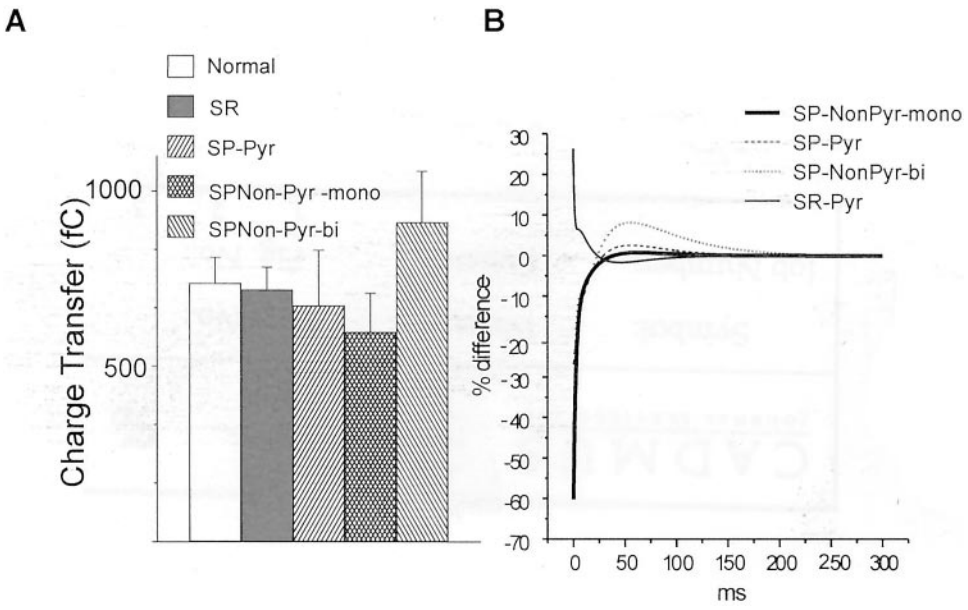

Figure 6. Comparison of the magnitude and time course of inhibition in the three strains. *A*, Calculated total charge transfer (holding potential, −60 mV; Cl^- reversal potential, ~0 mV) for averaged mIPSCs in various subpopulations, as described in Materials and Methods and shown in Figure 1. For normal and seizure-resistant strains, data shown are pooled between pyramidal (*Pyr*) and nonpyramidal (*Non-Pyr*) neurons. Despite differences in the peak amplitude of mIPSCs between the strains, there were no significant differences in the total charge transfer. *B*, Plot of deviations of average mIPSCs of the same subpopulations as above from the time course of the average mIPSC in normal rats. Data are presented as a percentage of the peak amplitude of the average mIPSC in normal rats. Inhibitory synapses in seizure-resistant (*SR*) rats pass more charge than those in normal rats over the first 10–20 msec. Synapses of seizure-prone (*SP*) rats, conversely, pass up to 50% less charge over the same time period compared with normal rats. These differences are compensated over the succeeding 100 msec to yield no net differences in charge transfer.

current than those in neurons from either seizure-resistant or normal rats. Likewise, synapses in seizure-resistant rats pass far more inhibitory current early than do either seizure-prone or normal rats. These differences suggest that the timing of synaptic deactivation is the most important functional difference in inhibitory signaling between the strains.

DISCUSSION

Our results demonstrate that inhibitory synaptic signals differ considerably in strains of rats that have different profiles of $GABA_A$ receptor subunit expression and concomitant genetic predispositions for or against kindling. Over the initial 20 msec time window, it is likely that these differences in timing are important for controlling the quality of the inhibition that closely follows an excitatory input to truncate excess action potential generation (i.e., inhibition that limits bursting). The significantly lower threshold for afterdischarge activity reported in the perirhinal cortex of seizure-prone versus seizure-resistant rats (McIntyre et al., 1999) probably reflects these differences in initial IPSC time course and amplitude. The increased magnitude of the inhibition during this epoch may then account primarily for the seizure-resistant phenotype, although other timing issues may play a role also (see below).

The strain-related differences we describe in synaptic deactivation kinetics correlate well with previously described differences in $GABA_A$ receptor subunit expression. Thus, in seizure-prone rats, in which the $\alpha3$ and $\alpha5$ $GABA_A$ receptor subunits are abundant, the observed slow deactivation profiles of mIPSCs are qualitatively similar to those in immature brain at a time when $\alpha3$ and $\alpha5$ levels are high (Brickley et al., 1996; Tia et al., 1996; Dunning et al., 1999; Hutcheon et al., 2000; Okada et al., 2000). Similarly, in the laterodorsal thalamus during ontogeny, the deactivation kinetics of inhibitory synapses speeds up as the $GABA_A$ subunit expression shifts from $\alpha2$ to $\alpha1$ forms (Okada et al., 2000). Moreover, the average monoexponential and biexponential kinetics of nonpyramidal (presumably inhibitory) neurons in the seizure-prone strain corresponds well to the average mIPSC kinetics in inhibitory neurons of the reticular nucleus of the adult thalamus (Huntsman and Huguenard, 2000), a structure with high $\alpha3$ expression (Fritschy and Mohler, 1995). Similar slow deactivation kinetics also has been described for cells expressing recombinant $\alpha5\beta3\gamma2$ receptors (Burgard et al., 1999). Monoexponential decays have been described for both $\alpha2$ and $\alpha3$ subunit-containing recombinant receptors (Gingrich et al., 1995; Lavoie et al., 1997; McClellan and Twyman, 1999). Likewise, in normal and seizure-resistant rats, the fast deactivation kinetics of $GABA_A$ receptors is similar to those in regions of the adult brain in which $\alpha1$ is the predominant $GABA_A$ receptor subunit (Galarreta and Hestrin, 1997). Thus, both in other studies and in our two genetic models of differential seizure susceptibility, there is a good correlation between the different expression patterns of $GABA_A$ receptor subunits and their associated synaptic kinetics.

On pyramidal neurons, we consistently found that peak mIPSC amplitudes in seizure-resistant rats were greater than in normal rats, which, in turn, were greater than those in seizure-prone rats. Because the single-channel conductance of $GABA_A$ receptors containing $\alpha\beta\gamma$ subunits appears to vary little with subunit expression (Neelands et al., 1998; Burgard et al., 1999; Haas and Macdonald, 1999), one possibility that may account for the small amplitudes of mIPSCs in seizure-prone rats may be a relative inability to efficiently cluster the particular subunit combinations they express. Indeed, our recent work shows that, during cortical development, $GABA_A$ synapses preferentially recruit receptors with fast kinetics (Hutcheon et al., 2000), presumably containing $\alpha1$ and not $\alpha3$ or $\alpha5$ receptor subunits (Poulter et al., 1997; Hutcheon et al., 2000). Similarly, a recent study by Vicini et al. (2001) has shown that knocking out the $\alpha1$ subunit prevents the functional maturation of inhibitory synapses characterized by the development of the fast phase of deactivation.

Thus, immature $\alpha3$ and $\alpha5$ subunits that are highly expressed in perirhinal cortex of seizure-prone rats may not be recruited efficiently into synapses, resulting in lower peak mIPSC amplitudes. Neurons may have specialized synaptic anchoring proteins for receptors containing the $\alpha1$ subunit and cannot efficiently harbor receptors with immature α subunit combinations. Conversely, the relatively larger amplitudes of mIPSCs observed in seizure-resistant rats are probably caused by synapses with higher than normal densities of $GABA_A$ receptors. This could simply reflect a higher abundance of the preferred $\alpha1$-containing recep-

tors available for inclusion in the synapses, because the α1 subunit is upregulated in the perirhinal cortex of seizure-resistant rats. Alternatively, the turnover rate of these receptors may be faster (in seizure-prone) or slower (in seizure-resistant), disfavoring or favoring the accumulation of receptors in synaptic sites.

It is thought that inhibitory networks play a central role in regulating neural network excitability and timing (Whittington et al., 1995; Wang and Buzsaki, 1996). In this context, we found major differences in the inhibitory synapses on nonpyramidal neurons in the seizure-prone rats, which may account for the previously reported strain differences in seizure genesis (Racine et al., 1999). Specifically, differences in the time course of inhibition on the interneurons in seizure-prone rats could have three effects that contribute to seizure genesis: (1) longer-lasting mIPSCs should summate more efficiently, leading to disinhibition of the principal cells and a collapse of network inhibition (Nusser et al., 1998); (2) more slowly decaying IPSCs on the nonpyramidal population would slow interneuron firing and thus slow the oscillations of the cortical networks (compared with normal or seizure-resistant rats), as reported for IPSCs on interneurons in the hippocampus (Whittington et al., 1995); and/or (3) strain-related timing differences in IPSCs could differentially interact with action potentials conveyed electrically through gap junctions to hamper or facilitate synchronous firing among interneurons (Tamas et al., 2000). It also interesting to note that the time course of summated inhibition is well matched between pyramidal and nonpyramidal neurons in both the normal and seizure-resistant rats but not in the seizure-prone rats. This suggests that a mismatch in inhibitory timing may favor seizure generation as well. Thus, inhibition in the seizure-prone and seizure-resistant strains has attributes that predict different timing patterns and efficacy of network entrainment and synchrony. However, because our results are correlative, like other reports on $GABA_A$ receptor expression and epilepsy (Shumate et al., 1998; Sperk et al., 1998; Brooks-Kayal et al., 1999; Loup et al., 2000), it is not known which if any of these mechanisms play a role in seizure genesis.

In summary, we have shown in seizure-prone rats, which normally kindle twice as fast as normal rats and up to 10 times faster than seizure-resistant rats (Racine et al., 1999), that $GABA_A$ receptor-mediated mIPSCs are smaller in amplitude but longer in time course than those in either normal or seizure-resistant rats. These differences are most pronounced in the nonpyramidal neurons of seizure-prone rats and the pyramidal neurons of seizure-resistant rats. These observations suggest, therefore, that the selective breeding has emphasized processes that localize and choose $GABA_A$ receptor subunits for insertion into synapses of perirhinal cortex excitatory and inhibitory neurons. Although these data are purely correlational, they still strongly suggest that one genetic fault responsible for fast epileptogenesis in the seizure-prone strain is the retarded development of expression of α subunits for the $GABA_A$ receptor, particularly on nonpyramidal neurons. It should be emphasized that the rats used in these studies were seizure free, and therefore, the observed differences speak primarily to the propensity to develop seizures and not necessarily to end points reflecting the epileptic state. Extrapolating from these data to humans suggests that the pathogenesis of TLE may be more related to the timing of GABAergic inhibition than to the total amount of inhibition received. Finally, in an important parallel observation, we have reported previously that our seizure-prone rats behaviorally exhibit deficits in attention, with mild hyperactivity and strong impulsivity, in a variety of tests (McIntyre and Anisman, 2000). Because attention-deficit hyperactivity with impulsivity in children is strongly associated with epilepsy (>20% of cases) compared with otherwise normal children (<2% of cases), the differences in inhibitory control shown here may point to the pathogenesis of other related disorders as well.

REFERENCES

Angelotti TP, Macdonald RL (1993) Assembly of $GABA_A$ receptor subunits: α1 β1 and α1 β1 γ2S subunits produce unique ion channels with dissimilar single-channel properties. J Neurosci 13:1429–1440.

Brickley SG, Cull-Candy SG, Farrant M (1996) Development of a tonic form of synaptic inhibition in rat cerebellar granule cells resulting from persistent activation of $GABA_A$ receptors. J Physiol (Lond) 497: 753–759.

Brooks-Kayal AR, Shumate MD, Jin H, Rikhter TY, Coulter DA (1998) Selective changes in single cell $GABA_A$ receptor subunit expression and function in temporal lobe epilepsy. Nat Med 4:1166–1172.

Brooks-Kayal AR, Shumate MD, Jin H, Lin DD, Rikhter TY, Holloway KL, Coulter DA (1999) Human neuronal $GABA_A$ receptors: coordinated subunit mRNA expression and functional correlates in individual dentate granule cells. J Neurosci 19:8312–8318.

Burgard EC, Haas KF, Macdonald RL (1999) Channel properties determine the transient activation kinetics of recombinant $GABA_A$ receptors. Brain Res Mol Brain Res 73:28–36.

Dominguez-Perrot C, Feltz P, Poulter MO (1995) Recombinant $GABA_A$ receptor desensitization: the role of the γ2 subunit and its physiological significance. J Physiol (Lond) 497:145–159.

Dunning DD, Hoover CL, Soltesz I, Smith MA, O'Dowd DK (1999) $GABA_A$ receptor-mediated miniature postsynaptic currents and alpha-subunit expression in developing cortical neurons. J Neurophysiol 82:3286–3297.

Ferland RJ, Nierenberg J, Applegate CD (1998) A role for the bilateral involvement of perirhinal cortex in generalized kindled seizure expression. Exp Neurol 151:124–137.

Fritschy JM, Mohler H (1995) $GABA_A$-receptor heterogeneity in the adult rat brain: differential regional and cellular distribution of seven major subunits. J Comp Neurol 359:154–194.

Galarreta M, Hestrin S (1997) Properties of $GABA_A$ receptors underlying inhibitory synaptic currents in neocortical pyramidal neurons. J Neurosci 17:7220–7227.

Gingrich KJ, Roberts WA, Kass RS (1995) Dependence of the $GABA_A$ receptor gating kinetics on the α-subunit isoform: implications for structure-function relations and synaptic transmission. J Physiol (Lond) 489:529–543.

Gloor P (1991) Neurobiological substrates of ictal behavioral changes. Adv Neurol 55:1–34.

Haas KF, Macdonald RL (1999) $GABA_A$ receptor subunit γ2 and δ subtypes confer unique kinetic properties on recombinant $GABA_A$ receptor currents in mouse fibroblasts. J Physiol (Lond) 514:27–45.

Huntsman MM, Huguenard JR (2000) Nucleus-specific differences in $GABA_A$-receptor-mediated inhibition are enhanced during thalamic development. J Neurophysiol 83:350–358.

Hutcheon B, Morley P, Poulter MO (2000) Developmental change in $GABA_A$ receptor desensitization kinetics and its role in synapse function in rat cortical neurons. J Physiol (Lond) 522:3–17.

Kelly ME, McIntyre DC (1996) Perirhinal cortex involvement in limbic kindled seizures. Epilepsy Res 26:233–243.

Lavoie AM, Tingey JJ, Harrison NL, Pritchett DB, Twyman RE (1997) Activation and deactivation rates of recombinant $GABA_A$ receptor channels are dependent on a α-subunit isoform. Biophys J 73:2518–2526.

Loup F, Wieser HG, Yonekawa Y, Aguzzi A, Fritschy JM (2000) Selective alterations in $GABA_A$ receptor subtypes in human temporal lobe epilepsy. J Neurosci 20:5401–5419.

McClellan AM, Twyman RE (1999) Receptor system response kinetics reveal functional subtypes of native murine and recombinant human $GABA_A$ receptors. J Physiol (Lond) 515:711–727.

McIntyre DC, Anisman H (2000) Anxiety and impulse control in rats selectively bred for seizure sensitivity. In: Contemporary issues in modeling psychopathology (Mysblodsky M, Weiner I, eds). New York: Kluwer Academic.

McIntyre DC, Kelly ME, Dufresne C (1999) FAST and SLOW amygdala kindling rat strains: comparison of amygdala, hippocampal, piriform and perirhinal cortex kindling. Epilepsy Res 35:197–209.

Neelands TR, Greenfield Jr LJ, Zhang J, Turner RS, Macdonald RL (1998) $GABA_A$ receptor pharmacology and subtype mRNA expression in human neuronal NT2-N cells. J Neurosci 18:4993–5007.

Nusser Z, Hajos N, Somogyi P, Mody I (1998) Increased number of synaptic $GABA_A$ receptors underlies potentiation at hippocampal inhibitory synapses. Nature 395:172–177.

Okada M, Onodera K, Van RC, Sieghart W, Takahashi T (2000) Func-

tional correlation of $GABA_A$ receptor α subunits expression with the properties of IPSCs in the developing thalamus. J Neurosci 20: 2202–2208.
Poulter MO, Ohannesian L, Larmet Y, Feltz P (1997) Evidence that $GABA_A$ receptor subunit mRNA expression during development is regulated by $GABA_A$ receptor stimulation. J Neurochem 68:631–639.
Poulter MO, Brown LA, Tynan S, Willick G, Williams R, McIntyre DC (1999) Differential expression of α1, α2, α3, and α5 $GABA_A$ receptor subunits in seizure-prone and seizure-resistant rat models of temporal lobe epilepsy. J Neurosci 19:4654–4661.
Racine R, Steingert MO, McIntyre DC (1999) Development of kindling-prone and kindling-resistant rats: selective breeding and electrophysiological studies. Epilepsy Res 35:183–195.
Schwartzkroin PA (1998) GABA synapses enter the molecular big time. Nat Med 4:1115–1116.
Shumate MD, Lin DD, Gibbs JW, Holloway KL, Coulter DA (1998) $GABA_A$ receptor function in epileptic human dentate granule cells: comparison to epileptic and control rat. Epilepsy Res 32:114–128.
Sperk G, Schwarzer C, Tsunashima K, Kandlhofer S (1998) Expression of $GABA_A$ receptor subunits in the hippocampus of the rat after kainic acid-induced seizures. Epilepsy Res 32:129–139.
Tamas G, Buhl EH, Lorincz A, Somogyi P (2000) Proximally targeted GABAergic synapses and gap junctions synchronize cortical interneurons. Nat Neurosci 3:366–371.
Tia S, Wang JF, Kotchabhakdi N, Vicini S (1996) Developmental changes of inhibitory synaptic currents in cerebellar granule neurons: role of $GABA_A$ receptor α6 subunit. J Neurosci 16:3630–3640.
Traub RD, Jefferys JGR, Whittington MA (1999) Fast oscillations in cortical circuits. Boston: MIT Press.
Verdoorn TA (1994) Formation of heteromeric γ-aminobutyric acid type A receptors containing two different α subunits. Mol Pharmacol 45:475–480.
Verdoorn TA, Draguhn A, Ymer S, Seeburg PH, Sakmann B (1990) Functional properties of recombinant rat $GABA_A$ receptors depend upon subunit composition. Neuron 4:919–928.
Vicini S, Ferguson C, Prybylowski K, Kralic J, Morrow AL, Homanics GE (2001) $GABA_A$ receptor α1 subunit deletion prevents developmental changes of inhibitory synaptic currents in cerebellar neurons. J Neurosci 21:3009–3016.
Wang XJ, Buzsaki G (1996) γ oscillation by synaptic inhibition in a hippocampal interneuronal network model. J Neurosci 16:6402–6413.
Whittington MA, Traub RD, Jefferys JG (1995) Synchronized oscillations in interneuron networks driven by metabotropic glutamate receptor activation. Nature 373:612–615.
Zhu WJ, Vicini S, Harris BT, Grayson DR (1995) NMDA-mediated modulation of GABA type A receptor function in cerebellar granule neurons. J Neurosci 15:7692–7701.